energies

MDPI

Review

Review of Studies on the Hot Spot Temperature of Oil-Immersed Transformers

Lin Lin [1,*], Chengdan Qiang [1], Hui Zhang [1,*], Qingguo Chen [1], Zhen An [2] and Weijie Xu [1]

[1] Key Laboratory of Engineering Dielectrics and Its Application, Ministry of Education, Harbin University of Science and Technology, Harbin 150080, China; 2220310165@stu.hrbust.edu.cn (C.Q.); qgchen@hrbust.edu.cn (Q.C.); 2420300053@stu.hrbust.edu.cn (W.X.)
[2] Wujiang Transformer Co., Ltd., Suzhou 215222, China; anzhen9605@163.com
* Correspondence: linlin_hrbust@163.com (L.L.); huizhang@hrbust.edu.cn (H.Z.); Tel./Fax: +86-0451-86391625 (L.L.)

Abstract: Oil-immersed transformers are the core equipment of power systems for energy transfer. The thermal characteristic of a transformer immediately affects its operational reliability and service life. Therefore, analyzing the hot spot temperature of transformers is highly important. Currently, researchers worldwide have achieved substantial research results in this field. This paper reviews the research status of the transformer hot spot temperature. First, the calculation method of transformer loss, the forms of heat transfer and its calculation method, the characteristics of the cooling method, and its application occasions are summarized. Second, the methods used to research the transformer hot spot temperature are presented in detail. From the perspective of transformer heat production and heat dissipation, research results on the factors influencing transformer hot spot temperature are summarized. Last, the research direction of the transformer hot spot temperature is indicated.

Keywords: transformer; hot spot temperature; loss calculation; heat transfer forms; cooling method

check for updates

Academic Editor: Ahmed Abu-Siada

Received: 30 November 2024
Revised: 20 December 2024
Accepted: 25 December 2024
Published: 28 December 2024

Citation: Lin, L.; Qiang, C.; Zhang, H.; Chen, Q.; An, Z.; Xu, W. Review of Studies on the Hot Spot Temperature of Oil-Immersed Transformers. *Energies* **2025**, *18*, 74. https://doi.org/10.3390/en18010074

Copyright: © 2024 by the authors. Licensee MDPI, Basel, Switzerland. This article is an open access article distributed under the terms and conditions of the Creative Commons Attribution (CC BY) license (https://creativecommons.org/licenses/by/4.0/).

1. Introduction

The distributions of primary energy and energy consumption centers are not balanced, which results in cross-regional, long-distance, and large-scale characteristics of electric power transmission [1]. Power transformers are the core equipment used in electric power transmission, among which oil-immersed transformers have strong load capacity and good insulation, accounting for approximately 67% of the large transformers that have been introduced into operation. Recently, oil-immersed transformers have accounted for approximately 85% of transformers; therefore, the operation status of oil-immersed transformers is directly related to the safety and stability of the power grid system [2]. With the rapid development of the national economy, the demand for a power supply is increasing, the voltage level of the power system is constantly increasing, and an increase in transformer capacity has become an essential requirement for the development of the power grid. Moreover, the impact of transformer failure increases. Therefore, ensuring the safe operation of power transformers is particularly important for the stable operation of power systems, industrial production, and people's daily lives.

During the operation of the transformer, a large amount of loss is generated and converted to heat, and most of the heat is absorbed by the transformer, increasing its internal temperature. With increasing transformer capacity, the electromagnetic loss of the

transformer increases, and the increase in electromagnetic loss is proportional to 3/4 square of the capacity. However, the size of the transformer does not increase commensurately, and the increase in the cooling area is proportional to 1/2 the capacity; therefore, the temperature increase problem of large-capacity transformers is more prominent [3]. There are two main effects of the increase in transformer temperature: on the one hand, increasing the transformer temperature causes internal local overheating, and local overheating results in deformation of the structure, which directly affects the safety of power transformer operation [4]; on the other hand, the increase in temperature affects the thermal aging rate of the transformer insulation materials. The national standard GB/T1094.7-2008 indicates that within the temperature range of 80–140 °C, the thermal aging rate of insulating materials follows the six-degree principle, with 98 °C as a hot spot temperature reference value, corresponding to the aging rate of insulating materials: every temperature increase of 6 °C causes a doubling of the aging rate. When the operating temperature is increased to 140 °C, the thermal aging rate is 128 times greater than that at an operating temperature of 98 °C, that is, the temperature increase accelerates the aging of the insulation material and greatly reduces the service life of the transformer [5,6]. In contrast, if the transformer hot spot temperature is too low, the transformer fails to fully utilize the load capacity, and the economic efficiency is reduced, resulting in a waste of resources. Therefore, research on the hot spot temperature of oil-immersed transformers can realize the rational design of transformers and improve their reliability; it can also effectively reduce the waste of energy in the power system and improve the economic index of the power grid. However, due to the transformer type, coil design, cooling method, and many other factors, it is still difficult to accurately determine the location of hot spot temperature and obtain its exact value by present research methods.

Based on the research status at home and abroad, this paper discusses the research results of oil-immersed transformer hot spot temperature in detail, summarizes transformer loss sources and calculation methods, analyzes the heat transfer mode of oil-immersed transformers and compares the characteristics of different cooling methods, summarizes research methods of transformer hot spot temperature, and reviews the influencing factors of hot spot temperature from the perspective of heat production and heat dissipation. This paper puts forward the key points on transformer cooling, points out the development direction of transformer hot spot temperature research method, and summarizes the methods of reducing hot spot temperature, with the goal of providing reference value and guidance for transformer research.

2. Transformer Heat Production

The transformer loss is the heat source of the corresponding temperature increase, which can be divided into core loss, winding loss, and stray loss caused by leakage of the magnetic field in the tank wall and structure.

2.1. Transformer Core Loss Research Status

The methods used to calculate iron core loss in the present study include the hysteresis loss modeling method, the empirical formula equivalence method, and the separation calculation method. The calculation method of iron core loss is shown in Table 1.

Table 1. Main research results and disadvantages of calculation methods of iron core loss.

Calculation Method	Author	Main Research Results	Disadvantages
Hysteresis loss modeling method	Preisach [7]	Proposed Preisach model, the magnetization of the dipole is obtained based on the time–space characteristics of the magnetic dipole, and the macromagnetization of the magnetic core is characterized by the sum of the magnetizations of the dipole.	When the hysteresis model is coupled with the magnetic field solution, the parameters need to change, and the model is very complicated under multi-factor.
	Jiles and Atherton [8]	Proposed Jiles–Atherton model, the principle of the balance between the movement of the magnetic domain wall and the macroscopic energy to calculate the magnetic core loss.	Based on many experimental results, and the difficulty in achieving the optimal design of the core under nonsinusoidal excitation.
Empirical formula equivalence method	Steinmetz [9–11]	Proposed an equivalent model of the empirical formula for the loss calculation of ferromagnetic materials, the model solves the problems of cumbersome application steps and complicated calculations.	The applicable frequency and submagnetic induction intensity range are small, and the calculation accuracy is low.
Separation calculation method	Bertotti [12]	Proposed a core loss separation calculation method applicable to sinusoidal and nonsinusoidal excitation.	
	Amar [13] and Boglietti [14]	Obtained the loss under the nonsinusoidal method by accumulating the loss results of each order of sinusoidal excitation.	
	Barbiso [15]	Realized parameter extraction on the basis of the linear relationship between the variables at different frequencies, and then realized the calculation of iron core loss.	
	Lavers [16]	Proposed a correction model of iron loss separation. Two correction factors, hysteresis loss correction and eddy current loss, were added to the model to obtain a more widely used model of iron core loss separation.	

Early researchers proposed the Preisach model, the Jiles–Atherton model, and other hysteresis loss models. Successively, researchers proposed an equivalent model of the empirical formula for the loss calculation of ferromagnetic materials, the empirical formula is shown in Formula as follows (1).

$$P_v = C_m f^{\alpha} B_m^{\beta} \tag{1}$$

where P_v is the core loss, f is the operating frequency, B_m is the amplitude of the magnetic induction density, and C_m, α, and β are the core coefficients.

According to the different generation mechanisms of ferromagnetic material losses, Bertotti proposed a core loss separation calculation method applicable to sinusoidal and

nonsinusoidal excitation and divided the core loss into three parts: hysteresis loss, eddy current loss, and residual loss [12]. The corresponding core loss calculation formula is shown in Formula as follows (2); researchers have subsequently proposed extended algorithms that are based on loss separation theory for realizing fast solutions of the core loss.

$$\begin{aligned} P_v &= P_h + P_{ce} + P_{ex} \\ &= C_h f B_m^{\alpha} + C_{ce} f^2 B_m^2 + C_{ex} f^{1.5} B_m^{1.5} \end{aligned} \tag{2}$$

where P_h is the hysteresis loss, P_{ce} is the eddy current loss, P_{ex} is the residual loss, and C_h, C_{ce}, C_{ex}, and α are the core coefficients.

Scholars from various countries have conducted a lot of research on the calculation of iron core loss. This paper shows the statistics calculation methods of iron core loss and summarizes the main research results and the disadvantages of the calculation methods, as shown in Table 1.

2.2. Transformer Winding Loss Research Status

The winding loss of the transformer refers to the loss of current flow through the winding and the loss caused by the leakage magnetic field in the winding and structural parts, including the loss generated by the DC resistance of the winding coil, the eddy current loss generated by the leakage flux in the winding, and the circulating current loss generated by the parallel winding of conductors. The resistance loss can be calculated directly via the formula according to the current and resistance values of the winding, and the circulating current loss is usually disregarded. Thus, the eddy current loss in the winding loss is a key concern of researchers. The calculation methods of winding eddy current loss include primarily analytical methods and finite element methods.

The analytical method is employed to reduce the dimensionality of the winding or simplify the processing, obtain analytic solutions according to Maxwell's equations, and then obtain the winding loss. The more classic analytic method is the one-dimensional analytical model published by Dowell [17]. Based on this model, Keradec et al. established an impedance network model that describes the conductor magnetic field strength and electric field strength [18], and a researcher subsequently investigated the applicability of this network model [19,20]. The analytical method requires simplification of the transformer structure, which has a low computational cost and can ensure calculation accuracy, but it is not applicable to the winding structure with cross transposition.

The finite element method calculates the winding loss by using the finite element method, which has high calculation accuracy and considers the nonlinearity of the material. Pang Xiaodong divided the leakage magnetic field into a longitudinal magnetic field and a transverse magnetic field and analyzed the distribution of the leakage magnetic field via finite element software. Combined with the eddy current loss calculation equation, the winding eddy current loss was calculated, and the results were compared with the value of the eddy current loss calculated via empirical equations. The accuracy of the calculation results was verified [21]. Wang Yuxiang used the finite element method to calculate the eddy current loss of transformer windings and input the calculation results into the winding temperature rise calculation equation. The calculation results and the winding temperature rise test results were compared to verify the accuracy of the finite element method [22]. Li Xin established a two-dimensional model of the transformer leakage magnetic field via finite element software to analyze the distribution of longitudinal and transverse magnetic fields on the surface of high- and low-voltage windings and accurately calculated the value of the eddy current losses of the windings, which was combined with the distribution of the magnetic field theoretically, and the accuracy of the calculated results was analyzed [23]. Pan Yapei used the finite element method to calculate the winding loss of a high frequency

switching power supply transformer, where the windings are composed of a single strand of heavy gauge wire and multiple strands of fine wire in parallel winding simulation analysis, and obtained the winding loss distribution [24]. Although the finite element method can calculate the winding eddy current loss with respect to various complex structures, it has a high computational cost.

2.3. Research Status of Transformer Stray Loss

Stray transformer loss is the loss generated by the leakage flux in the metal structure and the tank wall.

As early as the 20th century, Vasyutinsky proposed an analytical formula for calculating the stray losses in a structure [25]:

$$P_e = K\frac{fh^3(x_k\%)^2\Phi^2 \times 10^3}{5L(h+l-2r)^2} \tag{3}$$

where K is the empirical coefficient, h is the coil height, $x_k\%$ is the short-circuit impedance percentage, ϕ is the core flux per column, L is the perimeter of the tank, r is the radius of the winding, and l is the tank length.

The stray loss calculated via the analytical formula not only deviates from the actual measured value but also fails to reflect the loss distribution, so it is limited in practical applications. Currently, the stray loss calculation uses mainly the traditional finite element method and surface impedance method.

The distribution of magnetic induction intensity on the tank wall and structural parts is characterized by a large surface area and small internal depth area, so the eddy current loss is densely distributed within a penetration depth range (1–2 mm) on the tank wall and structural part surface. When the traditional finite element method is used to calculate transformer stray loss, it is necessary to stratify the grid division element reasonably to achieve higher calculation accuracy; thus, the calculation amount is large. The surface impedance method excludes the ferromagnetic material from the solution domain, uses its surface as the boundary of the solution domain, sets the surface impedance condition at the boundary, and solves the problem in the surface impedance equation, which avoids the difficulties associated with stratified analyses [26]. The surface impedance method is simple, and it can calculate transformer stray loss more quickly under the requirement of high accuracy, which offers high application value in engineering. Guerin C used the surface impedance method to calculate the eddy current loss of an oil tank, and compared with the finite element method, this method not only improved the accuracy of the calculation but also reduced the computation time [27]. Yan Bing used the surface impedance method to calculate the eddy current loss of the clamps and tie plates of a power transformer and compared the results with those of the finite element method. The results show that the calculation speed of the surface impedance method is much faster than that of the finite element method with the same calculation accuracy [28]. Zhao Zhigang used the numerical computing software to establish a three-dimensional transformer model. The surface impedance method and the finite element method were used to calculate transformer stray loss, and the TEAM P21-B model was used to construct a test system to measure stray loss. The measurement results were used to compare the accuracy of the calculation results. The results show that the calculation time of the surface impedance method is significantly reduced with the same calculation accuracy [29]. Liu Jianjun used the surface impedance method and the finite element method to calculate the TEAM Problem 2 model, and 3–11 h were required when the finite element method was used; however, the surface impedance method needed 1–3 min, so the calculation time was greatly reduced [30].

3. Transformer Heat Dissipation

3.1. Forms of Heat Transfer

The heat transfer forms of oil-immersed power transformers include heat conduction, heat convection, and heat radiation. The mode of heat transfer between parts of oil-immersed power transformer is shown in Figure 1.

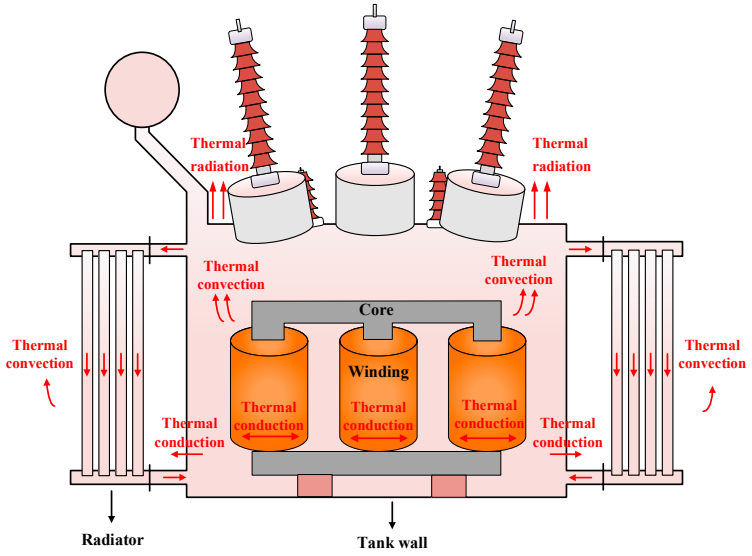

Figure 1. The mode of heat transfer between parts of oil-immersed power transformer.

(1) Thermal conduction

Thermal conduction is heat transfer in which heat is transferred from a hot object to a cold object in contact [31]. Thermal conduction occurs mainly in the heat transfer among the transformer core, the inside of the windings and their surfaces, and in the heat transfer among the transformer oil and the oil tank and radiator. The amount of heat transferred by conduction depends on the area of the contact surface of the object where the thermal conduction phenomenon occurs, the distance of heat conduction, and the temperature difference between the contact surfaces of the object [32], which is calculated as follows:

$$Q = S\lambda\frac{\Delta t}{l} \tag{4}$$

where Q is the heat transferred, S is the area of the contact surface of the object, λ is the thermal conductivity, Δt is the temperature difference between the surfaces of the object, and l is the heat conduction distance.

(2) Thermal convection

Thermal convection refers to the phenomenon of heat transfer caused by fluid flow [33]. Heat transfer occurs when a fluid contacts the solid surface of a transformer that has a relative temperature difference. Convective heat transfer occurs mainly in the heat transfer among the transformer core, windings and transformer oil, and in the heat transfer among the tank wall, radiator, and air. The amount of heat transferred by thermal convection is related to the properties of the fluid, the area of heat dissipation, and other factors [34], and the specific formula is as follows:

$$Q_\alpha = Sa(\theta_s - \theta_w) \tag{5}$$

where Q_a is the heat transferred by thermal convection, a is the heat transfer coefficient, S is the heat dissipation area, θ_s is the temperature of the cooled surface, and θ_w is the temperature of the cooling medium.

(3) Thermal radiation

Thermal radiation refers to the phenomenon in which a high-temperature object radiates electromagnetic waves to its surrounding low-temperature medium [35]. Thermal radiation in transformers occurs mainly in the heat transfer among the tank wall, the radiator, and its surrounding air. The heat emitted by thermal radiation is related to the surface area of the radiation, the temperature of the heating object and the heating medium, the energy radiated follows the Stefan–Boltzmann law [36], and the amount of heat transferred by thermal radiation can be calculated via the following formula:

$$Q = \varepsilon \delta S_A (\theta_1^4 - \theta_2^4) \tag{6}$$

where ε is the surface thermal emissivity, which is related to the material and surface area of the object; δ is the Stefan–Boltzmann constant, which is approximately 5.67×10^{-8} W/(m^2·K^4); S_A is the surface area of the radiation; θ_1 is the absolute temperature of the surface of the radiant body; and θ_2 is the absolute temperature of the medium around the radiant body.

3.2. Cooling Method

The internal temperature rise of the transformer depends on the internal heat generation and the heat dissipation ability of the transformer. In an oil-immersed transformer, insulating oil is the main cooling medium, and the heat generated by the core and windings dissipates into the surrounding medium. Figure 2 shows the internal oil flow path of the transformer.

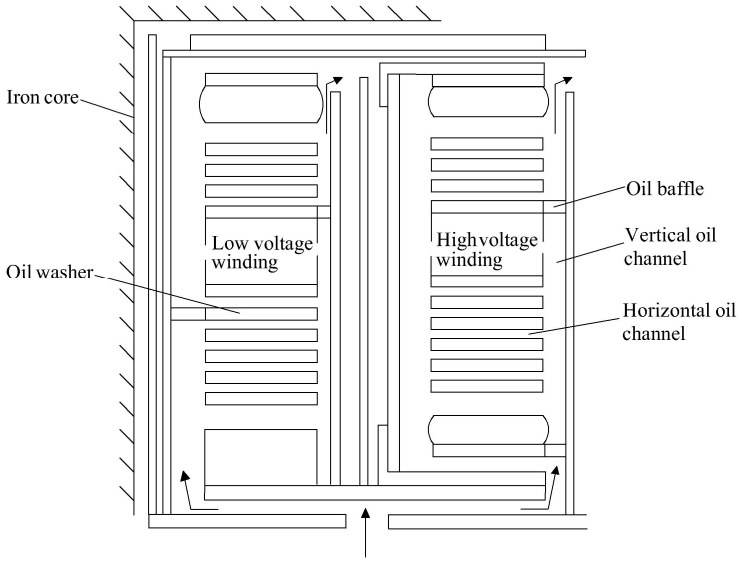

Figure 2. Diagram of internal oil flow path in oil-immersed transformer.

After the insulating oil absorbs heat, the temperature increases, the density decreases, and then the oil flows to the top layer due to the thermal buoyancy force. The insulating oil flow process causes heat transfer to the tank wall, the transformer oil density increases after heat is transferred out, the insulating oil flows back by gravity, and the transformer oil is reheated after contacting the heat source. This process is repeated throughout the cycles until the oil temperature in the transformer is consistent and thermal equilibrium

is achieved. To further improve the heat dissipation ability, heat pipes or radiators can be installed on the transformer box wall; for small- and medium-sized transformers, the above self-cooling heat dissipation method can meet the heat dissipation requirements. Therefore, a transformer with a small capacity uses the oil-natural air-natural (ONAN) cooling mode. For large-capacity transformers, to avoid an excessive internal temperature increase, improving the heat dissipation capacity of the transformer, that is, using different cooling methods, is necessary.

In addition to oil-natural air-natural cooling methods, transformer cooling methods also include oil-natural air-forced (ONAF) cooling, oil-forced air-forced (OFAF) cooling, oil-directed air-forced (ODAF) cooling, and oil-directed water-forced (ODWF) cooling. The comparison of the traditional cooling methods is shown in Table 2. In recent years, scholars at home and abroad have proposed a series of innovative heat dissipation technologies to improve the heat dissipation capacity of transformer radiator; for example, an external cooling module is installed to expand the heat dissipation area [37], and a spray device is added to take away more heat by means of phase change latent heat [38,39].

Table 2. Comparison of traditional cooling methods for oil-immersed transformers.

Cooling Method	Principle	Advantages/Disadvantages	Applicable Transformer Capacity and Voltage Class
ONAN [40]	Uses the density difference between transformer oil or air when it is heated or cooled to form natural convection and achieve a cooling effect [41].	Low noise level; there is no oil-flow electrification, but there is low efficiency.	≤5000 kVA, 110 kV; ≤31,500 kVA, ≤35 kV
ONAF [42]	Fans are added outside the radiator to force air convection, making the radiator achieve a more efficient cooling effect [43].	Higher cooling efficiency than ONAN; noise and oil-flow electrification problems are not as serious as those in forced-oil cooling.	12,500–63,000 kVA, 35–110 kV; ≤75,000 kVA, 110 kV; ≤40,000 kVA, 220 kV
OFAF [44,45]	A cooling method in which the oil is forced to circulate by a transformer oil pump to dissipate heat through a cooler [46].	High cooling efficiency; high noise, problem of oil-flow electrification, and limitation on oil flow speed (maximum of 0.5 m/s).	50,000–90,000 kVA, 220 kV; ≥60,000 kVA, ≥220 kV
ODAF/ODWF	On the basis of forced oil circulation, oil guide plates and other guiding structures are added to the winding oil channel to increase the oil flow rate and the cooling effect [47].	High cooling efficiency; noisy, obvious vibration, problem of oil-flow electrification.	≥75,000 kVA, 110 kV; ≥120,000 kVA, 220 kV; 330 kV; 550 kV

Table 2 shows that large-capacity transformers with a capacity greater than 60 MVA are cooled primarily by forced oil circulation, which improves heat dissipation by increasing the flow rate of insulating oil. However, when the insulating oil contacts the insulating paper, a double electrical layer will form. With the flow of insulating oil, the outer charge of the electric double layer is taken away by the oil flow to charge the insulating oil, which means that the phenomenon of oil-flow electrification occurs. The charge in the oil will accumulate on the surface of the insulating paper if the charge cannot be discharged in a timely manner. When the accumulated charge exceeds 40 nC, a discharge occurs, which affects the safe operation of the transformer. The problem of oil-flow electrification has become a major factor affecting the safe operation of 500 kV power transformers [48], and avoiding oil-flow

electrification is the key to improving heat dissipation in large-capacity transformers. The research shows that the flow rate of insulating oil, the type of electric field, and electric field strength are the key factors affecting the charged amount of oil flow [49]. At present, researchers mainly modify the insulating pressboard and insulating oil to inhibit oil-flow electrification, for example, nano-particle TiO_2 is added to the insulating pressboard, and benzotriazole (BTA) is added to the insulating oil. The effect of adding BTA in insulating oil on oil stream electrification is obviously better than that of adding nanomaterials in insulating paper; however, the effectiveness of BTA in insulating oil will decrease with time. Thus, the application of the modification method in the actual transformer remains to be researched [50].

4. Transformer Hot Spot Temperature Research Methods

4.1. Direct Measurement Method

The direct measurement method involves the installation of internal temperature sensors, which are connected to the measuring instrument, and the temperature of each point inside the transformer is directly measured by the measuring instrument [51,52]. Direct measurement methods initially used infrared, acoustic frequency, or other traditional temperature sensors to measure transformer hot spot temperatures; currently, the methods are relatively mature. However, owing to the occurrence of electromagnetic interference during the operation of oil-immersed transformers, the insulating oil of a transformer is also aged by oxidation, high temperature, humidity, and other environmental factors. Moreover, traditional temperature sensors operate in poor working environments, cannot accurately measure the temperature inside the transformer, can measure only the temperature on the surface of the tank and the external surface of the transformer, and the measurement results are affected by electromagnetic interference and the influence of the external environment [53,54].

In the 1970s, researchers began to measure the temperature of transformer hot spots via fiber optic temperature sensors [55–57]. An optical fiber temperature sensor uses the relationship between the light absorption and temperature of the semiconductor material to measure the temperature by detecting the light intensity reflected by the semiconductor material through a light detector [58–61]. In 1979, for the first time, researchers used the first generation of fluorescent fiber sensors for transformer internal temperature detection. The size of these fluorescent fiber optic sensors is suitable for mounting on the inside of power transformers. However, these materials are not guaranteed to be useful for long periods in oil-immersed transformer environments [62]. In 2004, Shin SiJin proposed a fiber Bragg grating temperature sensor using stainless steel thin tube encapsulation and pretension, which not only improved the sensitivity of the temperature sensor but also maintained good repeatability and linearity [63]. In 2008, Ribeiro A B L et al. proposed a fiber Bragg grating sensor encapsulated by a special quartz capillary and PTFE to construct a multipoint fiber optic sensing system for hot spot temperature measurement of power transformers. The temperature monitoring system based on fiber Bragg grating sensor is shown in Figure 3. The system had a total of 12 temperature sensing points distributed in the transformer's internal winding, cooling oil inlet and outlet, etc. The overall accuracy reached ±1 °C [64]. In 2011, Qi Yaobin proposed a fiber Bragg grating sensor encapsulated by a thin sheet of aluminum plate. Compared with that of the bare fiber grating, the sensitivity was greatly improved, the measurement was accurate, and the linearity was retained. Owing to the high voltage and strong magnetic field of the operating environment inside the transformer, the metal-encapsulated grating fiber optic sensor readily encounters interference when the internal temperature of the transformer is measured [65]. In 2017, Wang En proposed a fiber Bragg grating temperature sensor encapsulated by high-temperature

and corrosion-resistant PTFE material, which can be used for direct measurement of the transformer's internal temperature [66]. Fiber optic sensors are smaller and lighter than traditional temperature sensors, and the measurement is less affected by high voltage and electromagnetic interference [67–71]. Fiber optic sensors solve the problem that traditional temperature sensors cannot detect the internal temperature of a transformer, and their application in transformer temperature measurement is gradually increasing [72–74]. The optical fiber detection system has been applied in engineering; the measurement range is 0–200 °C, the resolution is 0.5 °C, the accuracy is ±2 °C, and the system is widely used in a variety of transformers. The accuracy of the fiber-optic sensor temperature detection results is affected by the thermal stress of the winding, the electromotive force, and the oil flow perturbation. In addition, because the hot spot position cannot be determined, there is a deviation between the measured position and the hot spot position. Future research on optical fiber temperature measurement technology will focus on resisting electromagnetic interference, withstanding high voltage, and improving sensitivity.

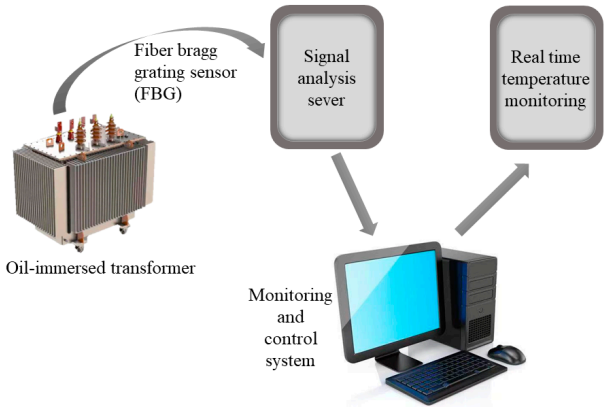

Figure 3. Temperature monitoring system based on a fiber Bragg grating sensor.

4.2. Indirect Calculation Method

Indirect calculation methods include the empirical formula method, the thermal circuit modeling method, and the numerical calculation method.

(1) Empirical formula method

The empirical formula method was the early calculation method for the transformer temperature. The definition of the hot spot temperature was first proposed by Cooney W. H. in 1925 [75]. Currently, for the calculation of transformer hot spot temperature, the transformer hot spot temperature calculation model, as recommended in IEEE Standard C57.91-2011 [76] and national standard GB/T 1094.7-2008 (corresponding to IEC 60076-7:2005), which is more commonly used [5,77]. Figure 4 shows a diagram of transformer heat distribution in GB/T 1094.7-2008.

The transformer oil temperature linearly increases from the bottom of the tank to the top of the tank, and the variation in temperature is not affected by the cooling method. The temperature of the winding wire increases from the bottom up and is parallel to the transformer oil temperature. The calculation formula for the transformer hot spot temperature is as follows:

$$\theta_{hst} = \theta_{oil} + H \times g_r \quad (7)$$

where H is the hot spot coefficient, which is related to the transformer capacity, short-circuit impedance, and winding structure. For distribution transformers, H is 1.1; for medium and large transformers, H is 1.3; and g_r is the distance between the two parallel lines in the above figure.

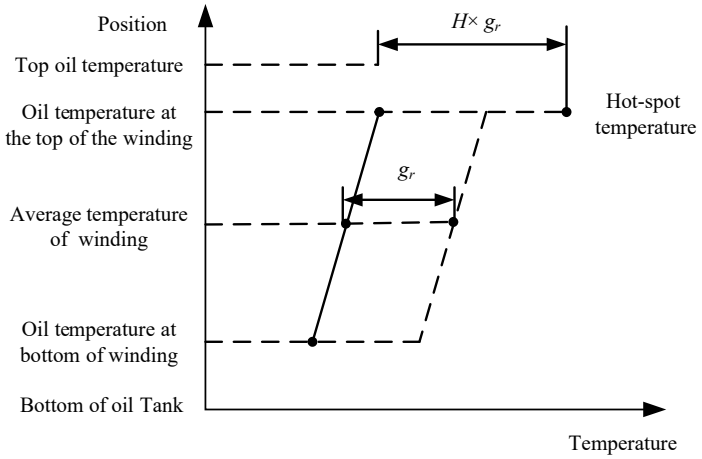

Figure 4. Diagram of transformer heat distribution in GB/T 1094.7-2008.

To simplify the complex situation in the transformer, this method assumes that the temperature increase of the winding from the bottom to the top is linear, but the hot spot temperature of the winding is not at the top of the winding in the transformer temperature rise test. This assumption is not consistent with reality, so there is a certain difference between the results calculated via the transformer hot spot temperature model on the basis of empirical formulas and the actual measurement results, which cannot reflect the transformer internal temperature change.

(2) Thermal circuit modeling method

In 2001, Swift et al. proposed a thermal circuit model based on the top oil temperature, which equates the heat transfer process inside the transformer to a circuit, where the amount of heat generated in the transformer corresponds to the current in the circuit, the temperature corresponds to the voltage in the circuit, the thermal resistance corresponds to the resistance in the circuit, and the thermal capacitance corresponds to the capacitance in the circuit [78,79]. As shown in Figure 5, the two current sources q_{cu} and q_{fe} are the input losses (copper loss and iron loss, respectively); the resistors R_{oil} and R_{wnd} are the thermal resistance of the insulating oil and the thermal resistance of the windings, respectively; the voltage source θ_{amb} is the external ambient temperature; and the capacitance C_{oil} is the thermal capacity of the insulating oil [80]. The differential equation for the equivalent circuit shown in the figure below is as follows:

$$q_{fe} + q_{cu} = C_{oil} \cdot \frac{d\theta_{oil}}{dt} + \frac{1}{R_{oil}} \cdot (\theta_{oil} - \theta_{amb})^{\frac{1}{n}} \tag{8}$$

where the value of n is related to the cooling method, n is 0.8 for natural oil cooling, and n is 1 for forced oil cooling.

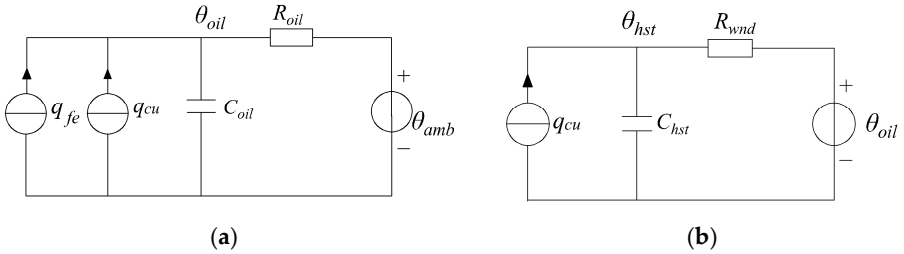

Figure 5. Transformer thermal circuit model based on the top oil temperature: (**a**) thermal circuit model of the top oil temperature and ambient temperature and (**b**) thermal circuit model of the hot spot temperature and ambient temperature.

In 2009, on the basis of the theory proposed by Pierece S L, Jiang Taosha et al. established a thermal circuit model based on the bottom oil temperature. After experimental verification, the transformer hot spot temperature can be accurately calculated via this model [81,82].

The hot spot temperature research method, which is based on a thermal circuit model, has a low calculation cost. However, because the lumped parameters are used, the transformer is regarded as a whole, the shape of the winding cake is disregarded, and some parameters are not accurate. Its accuracy depends on the selection of parameters such as the thermal resistance, heat capacity and heat source, and the temperature distribution inside the transformer cannot be obtained. In addition, the parameters of the thermal circuit model change when the transformer structure is different; therefore, this transformer hot spot temperature research method is applicable in the calculation of the hot spot temperature of power transformers with common structures.

(3) Numerical simulation method

The numerical simulation method is used to calculate the temperature field of a transformer by establishing a transformer model and using numerical calculation methods such as the finite element method, finite difference method, and finite volume method [83–85]. In 2009, Taghikhani M A utilized the finite element method to establish a numerical calculation method based on thermal conduction theory to obtain the temperature distributions of nondirectional oil-cooled and directional oil-cooled transformer windings [86]. In 2011, Chen Weigen solved flow–solid coupled convective heat transfer control equations by establishing a numerical model of the finite volume method to obtain the temperature distribution of the transformer winding; compared with the experimental prototype, the average relative error was 5.8% [87]. In 2012, Tsili M A established a three-dimensional finite element model of the coupled flow-thermal field, and the model accuracy was improved as much as possible under the premise of controlling the minimum amount of computation and realizing the prediction of the thermal distribution of the transformer [88]. In 2014, Wang Yongqiang proposed a hybrid computational method that combines the advantages of both the finite difference method and the finite volume method. The calculation results of the three-dimensional hot spot temperature of the transformer revealed that the hybrid algorithm is more accurate than the two methods alone [89]. In 2022, Li Jianxun established a two-dimensional model of a converter transformer via the finite element method, and the distributions of its internal temperature field and flow field were obtained by coupling calculations of the magnetic field, flow field, and hot spot temperature [90]. In 2023, Yuan Fating established a three-dimensional model of a transformer with a voltage of 35 kV, and the distributions of the transformer temperature field and flow field were obtained through fluid–thermal coupling calculations of the transformer hot spot temperature and flow field distribution. According to the simulation results, the hot spot temperature and structural parameters, the optimal structural parameters of the radiator were obtained, and the optimization results revealed that the hot spot temperature of the transformer decreased significantly [91].

The results of the numerical simulation are intuitive, and the temperature distribution inside the transformer can be obtained. With improvements in the numerical calculation level and simulation software upgrades, the temperature field distribution of transformers obtained via the numerical simulation method has become increasingly close to the real temperature field distribution. Because the flow of transformer oil is quite complex and the calculation capacity of computers is limited, the accuracy of the mesh becomes asymptotic, and the simplified model is often used in transformer simulations, making the results of the numerical calculation method deviate from the actual values.

(4) Artificial intelligence algorithm

Artificial intelligence algorithm is based on the strong computing power of intelligent algorithms. According to the real-time monitoring information of the transformer, the mechanism relationship between characteristics of temperature rise and influencing factors is established through data mining and then used for the prediction of hot spot temperature [92].

In order to predict the hot spot temperature of the transformer, Wang Jian divided the hot spot temperature, load coefficient, and ambient temperature measured by the transformer into a training set and a prediction set. A genetic programming algorithm was used to model the training set, and then an explicit prediction model that can evaluate the dynamic hot spot temperature was established [93].

Yang Chun proposed a hot spot temperature prediction method based on an improved BP neural network. The data samples were pre-processed by an improved principal component analysis method, and the initial weights and thresholds were optimized by the ant colony algorithm to improve the network performance and prediction accuracy [94].

SIMA Wenxia obtained hot spot temperature training samples under different ambient temperatures and load conditions through fluid-thermal coupling simulation calculation and built deep learning models using a long short-term memory network (LSTM) to achieve dynamic prediction of hot spot temperature [95].

4.3. Comparison of Transformer Hot Spot Temperature Research Methods

In view of the large number of hot spot temperature research methods, due to the methods based on different principles of measurement or calculation, each research method has corresponding adaptability and limitations. The comparison of various research methods is shown in Table 3. In practical engineering, researchers should flexibly choose the method according to the scene. With the development of intelligent algorithms, some achievements have been made in transformer temperature prediction and load prediction, but the hysteresis problem in model prediction and the improvement of accuracy of model prediction still need further research.

Table 3. Comparison of research methods for hot spot temperature.

Measurement Method	Classification	Advantages	Suitable for Application	Disadvantages
Direct measurement method	Temperature sensors	Highest precision	Little change in the transformer load.	Difficult to implement; Affected transformer internal insulation performance; It is difficult to locate the hot spot of the transformer.
	Fiber optic temperature sensors			
Indirect calculation method	Empirical formula method	Data is easily obtained; Easy to implement.	Low precision requirement.	Large error.
	Thermal circuit modeling method	Low calculation cost; Simple and very straightforward to use.	Power transformers with common structures; Study on nonlinear thermal characteristics of transformers.	Getting parameters requires a lot of offline testing.

Table 3. *Cont.*

Measurement Method	Classification	Advantages	Suitable for Application	Disadvantages
Indirect calculation method	Numerical simulation method	Whole temperature distribution of the transformer can be calculated; Result is very close to the real operating condition.	Characteristics of transformer internal temperature distribution were analyzed.	Time-consuming long; Complex modeling and low generality; Require computer with massive processing power. The Accuracy affected by model establishment and boundary condition setting.
	Artificial intelligence algorithm	High speed, high efficiency and high precision	Shows very strong practicability and superiority in hot spot temperature prediction.	Prediction accuracy is affected by the topological structure of the model, the selection of input parameters and the reliability of the training samples.

5. Factors

5.1. Factors Influencing Heat Production

Losses are the thermal sources of the transformer hot spot temperature. In large power transformers, the losses caused by leakage magnetic fields account for up to 30–40% of the total losses. The leakage magnetic field will cause eddy currents in structural parts, such as the pulling plate and the clamp, resulting in local overheating of the structural parts. In the 1980s, researchers focused on the factors influencing the leakage magnetic distribution. With the development of the three-dimensional finite element method, the study of the leakage magnetic field and loss has increased in depth. To limit the increase in transformer temperature, methods to reduce eddy current loss have been proposed. The eddy current loss is reduced mainly by adjusting the size of the structural parts and adopting magnetic shielding [96–98].

To adjust the size of the structure, Li Lin used the surface impedance method to calculate the three-dimensional nonlinear leakage magnetic field of the transformer and the eddy current loss of the transformer core pull plate. Moreover, the eddy current loss and maximum temperature increase of the pull plate for different sizes, numbers of slots, and load currents are calculated. The results show that the eddy current loss and the maximum temperature increase of the pull plate are positively correlated with the width of the core pull plate; the eddy current loss and the maximum temperature increase of the pull plate decrease with increasing number of slots and increase approximately linearly with increasing load current [99]. Gong Lina analyzed the effect of the slot size of the pull plate on the transformer eddy current loss, and the simulation results revealed that the eddy current loss decreases significantly when the length and width of the slotting of the tie plate increase [100]. In terms of magnetic shielding, Li Yan established a three-dimensional coupling model of the magnetic field and thermal field, calculated the eddy current loss generated by the leakage magnetic field in the tank and clamps, and analyzed the effects of the size of the shielding structure on the eddy current loss and the hot spot temperature increase. Research has shown that with increasing height of the magnetic shielding of the fuel tank, the eddy current loss and temperature increase decrease and then tend towards stability; the eddy current loss decreases with increasing length of the magnetic shielding of the fuel tank and height of the magnetic shielding of the clamps; and with increasing magnetic shield length of the clip, the eddy current loss decreases and then essentially remains unchanged [101]. Hu Yan analyzed the effects of the number of lead parallel conductors, the structure of the copper shield, and the magnitude of the lead

current on the magnetic leakage field of the oil tank. The results show that the magnetic leakage field distribution can be effectively improved when the lead wire is connected in parallel and when the minimum thickness of the copper plate is 4 mm. The maximum loss density increases when the thickness of the cover increases and the lead current increases. Therefore, the design should decrease the thickness of the elevated seat cover as much as possible while also reducing the lead current [102]. Ho S L analyzed the eddy current field distribution of current leads and windings, reported that the use of a high-permeability steel plate as a scaleboard can significantly reduce the eddy current loss of the flange, and proposed that the installation of a magnetic bypass plate can provide a path for leakage flux, which can reduce the leakage magnetic field in the clamp plate and the pull plate [103]. In 2012, Jing Yongteng analyzed the effects of different magnetic shielding methods on the eddy current field and reported that the eddy current loss of an oil tank was significantly reduced after installing tank magnetic shielding. Lung-type magnetic shielding and L-type magnetic shielding can significantly reduce the eddy current loss of clamps, and all three types of shielding methods can effectively reduce the total eddy current loss in a structure [104].

5.2. Heat Dissipation Factors

The amount of heat dissipation of the transformer depends on the heat dissipation environment and the ability of the cooling system to dissipate heat.

The change of ambient temperature will affect the heat dissipation of the entire transformer, reducing the ambient temperature can increase the temperature difference between the transformer tank and the air, driven by the temperature gradient, the heat exchange between the transformer and the surrounding environment is more frequent, and the hot spot temperature will be reduced; the research shows that the hot spot temperature decreases linearly with the reduction of the ambient temperature [105]. For most transformers in the power system, the ambient temperature is the atmospheric temperature, so it is impossible to improve the heat dissipation capacity by adjusting the ambient temperature.

If the ambient temperature is certain, the heat dissipation capacity of the transformer cooling system determines the hot spot temperature. The cooling system heat dissipation capacity can be improved mainly from two aspects. On the one hand, it is to improve the thermodynamic properties of transformer insulation materials. On the other hand, it is to change the flow state of the cooling medium and adjust the structure and layout of the cooling device.

The main means to improve the thermodynamic properties of transformer insulation materials include the modification of insulation materials or the use of new insulation materials with high thermal conductivity and high thermal capacity. In order to optimize the heat dissipation performance of transformer oil, the researchers uniformly dispersed nano-metal or non-metallic oxide particles into transformer oil to form nano-fluids. The research shows that nano-fluids can enhance heat transfer significantly, which can increase the thermal conductivity of transformer oil by 8% and the overall heat transfer efficiency by 20% [106,107]. The higher the thermal conductivity of insulating oil, the more conducive to energy transfer so that the heat in the transformer can be dissipated rapidly to reduce the hot spot temperature. Later, researchers applied the modified method to improve the performance of insulating paperboard, and the modified insulating paper showed significant improvement in thermal aging performance [108]. Although the addition of nanomaterials improves the thermodynamic properties of insulating materials, nanomaterials will aggregate or fall off under the action of gravity field or other force fields, which makes it difficult to maintain long-term stability, limiting the application of modified insulating materials. In addition, researchers used new insulating media with high thermal conductivity and high

thermal capacity, including synthetic fiber insulating materials, natural ester oil, etc. [109]. Natural ester oil has a higher thermal conductivity than mineral oil, and natural ester oil has been applied in transformers [110]. In 2021, the first 220 kV/240 MVA natural ester-insulated oil transformer developed by China XD Group successfully passed the type test and was officially put into operation [111]. However, the mechanical properties of synthetic fiber insulating materials are low, and the manufacturing cost is high; in addition to some applications of aramid insulating paper, the rest of the synthetic fiber paper has not been put into industrial production [108].

Transformers utilize cooling systems to dissipate heat, and the cooling efficiency of transformers can be improved by adjusting the oil flow state and the structure and arrangement of the cooling device. As a cooling medium, the flow state of insulating oil has a significant impact on the hot spot temperature of the transformer winding. The flow state of insulating oil can be adjusted by changing the oil flow velocity and the oil channel structure. Figure 6 shows the influence law of the oil flow velocity and oil channel structure on the hot spot temperature of the winding. The figure shows that the hot spot temperature of the transformer winding decreases with increasing oil flow velocity and inlet oil channel width but increases with increasing vertical oil channel width [112–114], as shown in Figure 6a,b. The reason for this is that the increase in the oil flow velocity and widening of the oil channel inlet width result in an increased insulating oil flow rate, making the insulating oil remove more heat per unit of time so that the hot spot temperature of the winding decreases. When the insulating oil flow rate is constant, widening the vertical oil passage width reduces the insulating oil flow speed and reduces heat dissipation and the hot spot temperature of the winding increases, as shown in Figure 6c. The installation of the oil baffle plate in the oil channel can control the flow path of transformer oil, and the influence of the number of oil baffle plates on the hot spot temperature of the windings is shown in Figure 6d. A reasonable arrangement of the oil baffle plate can eliminate stagnation of the oil flow in the horizontal oil channel, improve the distribution of the oil flow, and thus increase the efficiency of heat dissipation; however, an excessive number of baffles increases the resistance of insulation oil flow. At this point, increasing the number of baffles increases the hot spot temperature, so as the number of baffle plates increases, the hot spot temperature of the transformer increases and then decreases [113]. The height of the horizontal oil channel also affects the flow of the insulating oil: the higher the position of the horizontal oil channel is, the lower the resistance of the insulating oil to downwards flow. Therefore, the hot spot temperature of the windings decreases with increasing height of the horizontal oil channel, as shown in Figure 6e. In addition, when the number and width of gaskets between windings increase, the flow rate of insulating oil is limited, and the hot spot temperature of windings increases; similarly, when the number of discs is certain, the hot spot temperature of the winding increases with increasing number of discs between the gaskets [114,115].

The cooling capacity of the cooler strongly influences the temperature rise of the transformer. Researchers have conducted many studies on the cooler structure and internal flow field characteristics. Research has focused mainly on optimizing the cooler fin structure, improving the fin arrangement and adjusting the cooler arrangement and relative position. The optimization of the fin structure and reasonable fin arrangement can expand the heat transfer area and disturb the fluid to promote turbulence to improve the heat dissipation capacity of the cooler [116–119]. Adjusting the arrangement and relative position of the cooler can effectively improve the flow distribution characteristics so that the insulating oil can more quickly reach the top layer of the tank from the bottom layer of the tank, thus achieving a better cooling effect [115,120].

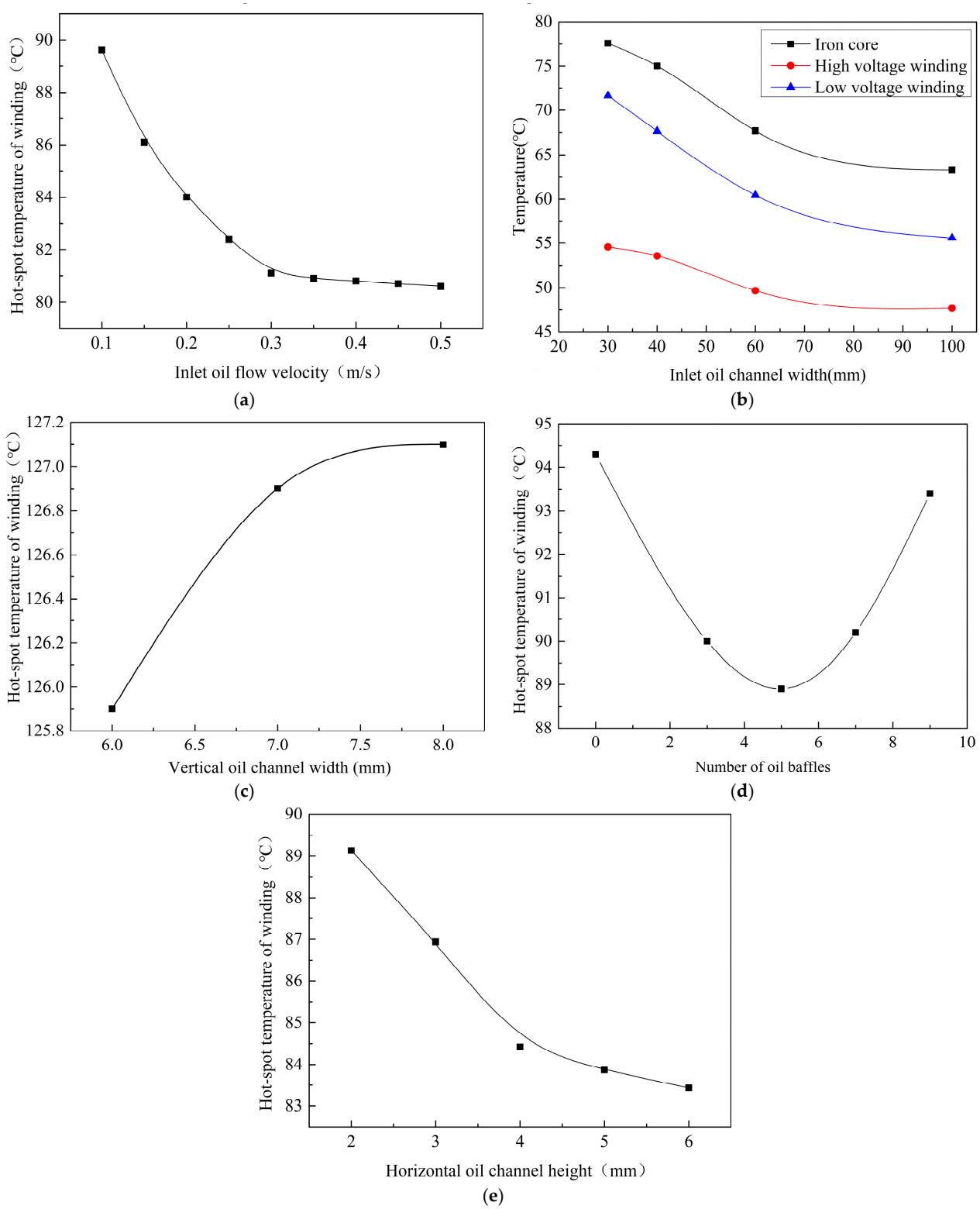

Figure 6. Influence of the oil flow state and oil channel structure on the hot spot temperature of the winding: (**a**) influence of the inlet oil flow velocity, (**b**) influence of the inlet oil channel width, (**c**) influence of the vertical oil channel width, (**d**) influence of the number of oil baffles, and (**e**) influence of the horizontal oil channel height.

6. Conclusions

This paper reviews the relevant results of domestic and foreign researchers in the field of transformer hot spot temperature research from the two aspects of transformer heat

generation and heat dissipation, summarizes the research results achieved worldwide from four aspects of heat generation inside the transformer, including heat dissipation, hot spot temperature research methods and hot spot temperature influencing factors, and obtains the following conclusions:

(1) Large transformers use the forced oil circulation cooling method to increase heat dissipation; when the oil flow velocity is too high, oil flow electrification will occur, damaging transformer insulation. Therefore, it is necessary to explore the mechanism of oil flow electrification and propose measures to restrain oil flow electrification, which is an urgent problem for improving the heat dissipation capacity of large-capacity transformers.

(2) With the development of intelligent algorithms, some achievements have been made in transformer temperature prediction and load prediction, but the hysteresis problem in model prediction and the improvement of the accuracy of model prediction still need further research.

(3) The temperature increase of the transformer can be reduced by reducing the transformer heat production or improving the transformer heat dissipation ability. Adjusting the size of the transformer structure and increasing the magnetic shield can effectively reduce the eddy current loss and reduce the heat production of the transformer. The heat dissipation capacity of the transformer can be achieved by increasing the insulation oil flow, optimizing the oil channel structure, adjusting the arrangement of the cooler, etc., to improve the hot spot temperature distribution of the transformer.

Author Contributions: Conceptualization, L.L. and H.Z.; investigation, L.L., C.Q. and Z.A.; data curation, L.L. and C.Q.; writing—original draft preparation, L.L. and C.Q.; writing—review and editing, L.L., C.Q. and W.X.; visualization, L.L. and C.Q.; supervision, Q.C. and H.Z. All authors have read and agreed to the published version of the manuscript.

Funding: This research received no external funding.

Conflicts of Interest: Author Zhen An was employed by the Wujiang Transformer Co., Ltd. The remaining authors declare that the research was conducted in the absence of any commercial or financial relationships that could be construed as a potential conflict of interest.

References

1. Liu, Z.; Zhang, Q. Study on the development mode of national power grid of China. *Proc. CSEE* **2013**, *33*, 1–10.
2. Luo, C. Study on Spatial Thermal Circuit Model and Temperature Characteristics of Oil-Immersed Transformer. Doctoral Dissertation, Kunming University of Science and Technology, Kunming, China, 2023.
3. Lu, C. *Power Transformer Theory and Calculation*, 4th ed.; Liaoning Science and Technology Publishing House: Shenyang, China, 2007.
4. Li, S. On Line Prediction Technology for Inner Winding Temperature Rise of EHV Power Transformer. Master's Thesis, Changchun University of Technology, Changchun, China, 2018.
5. *GB/T 1094.7-2008*; Power Transformers—Part 7: Loading Guide for Mineral-Oil-Immersed Power Transformers. China National Standards: Beijing, China, 2008.
6. Wu, J. Effect of Partial Overheating on Discharge Characteristics of Oil. Master's Thesis, Southwest Jiaotong University, Chengdu, China, 2019.
7. Bernard, Y.; Mendes, E.; Bouillault, F. Dynamic hysteresis modeling based on Preisach model. *IEEE Trans. Magn.* **2002**, *38*, 885–888. [CrossRef]
8. Jiles, D.; Atherton, D. Ferromagnetic hysteresis. *IEEE Trans. Magn.* **1983**, *19*, 2183–2185. [CrossRef]
9. Steinmetz, C.P. On the law of hysteresis. *Proc. IEEE* **1984**, *72*, 197–221. [CrossRef]
10. Muhlethaler, J.; Biela, J.; Kolar, J.W.; Ecklebe, A. Improved core-loss calculation for magnetic components employed in power electronic systems. *IEEE Trans. Power Electron.* **2011**, *27*, 964–973. [CrossRef]
11. Reinert, J.; Brockmeyer, A.; De Doncker, R.W. Calculation of losses in ferro-and ferrimagnetic materials based on the modified Steinmetz equation. *IEEE Trans. Ind. Appl.* **2001**, *37*, 1055–1061. [CrossRef]

12. Bertotti, G. General properties of power losses in soft ferromagnetic materials. *IEEE Trans. Magn.* **1988**, *24*, 621–630. [CrossRef]
13. Amar, M.; Kaczmarek, R. A general formula for prediction of iron losses under nonsinusoidal voltage waveform. *IEEE Trans. Magn.* **1995**, *31*, 2504–2509. [CrossRef]
14. Boglietti, A.; Cavagnino, A.; Lazzari, M.; Pastorelli, M. Predicting iron losses in soft magnetic materials with arbitrary voltage supply: An engineering approach. *IEEE Trans. Magn.* **2003**, *39*, 981–989. [CrossRef]
15. Barbisio, E.; Fiorillo, F.; Ragusa, C. Predicting loss in magnetic steels under arbitrary induction waveform and with minor hysteresis loops. *IEEE Trans. Magn.* **2004**, *40*, 1810–1819. [CrossRef]
16. Lavers, J.; Biringer, P.P.; Hollitscher, H. A simple method of estimating the minor loop hysteresis loss in thin laminations. *IEEE Trans. Magn.* **1978**, *14*, 386–388. [CrossRef]
17. Dowell, P.L. Effects of eddy currents in transformer windings. *Proc. Inst. Electr. Eng.* **1966**, *133*, 1387–1394. [CrossRef]
18. Keradec, J.P.; Cogitore, B.; Blache, F. Power transfer in a two-winding transformer: From 1-D propagation to an equivalent circuit. *IEEE Trans. Magn.* **1996**, *32*, 274–280. [CrossRef]
19. Schellmanns, A.; Fouassier, P.; Keradec, J.P.; Schanen, J.L. Equivalent circuits for transformers based on one-dimensional propagation: Accounting for multilayer structure of windings and ferrite losses. *IEEE Trans. Magn.* **2000**, *36*, 3778–3784. [CrossRef]
20. Tria, L.A.R.; Zhang, D.; Fletcher, J.E. Planar PCB transformer model for circuit simulation. *IEEE Trans. Magn.* **2016**, *52*, 1–4. [CrossRef]
21. Pang, X. The Study of the Eddy Losses and Temperature Field of Winding in Power Transformer. Master's Thesis, Hebei University of Technology, Tianjin, China, 2006.
22. Wang, Y.; Wang, J.; Liu, J.; Zhao, Y.; Li, H.; Li, Z. Research on Winding Eddy Loss and Temperature Rise Distribution for Oil immersed Transformer. *Electr. Power Sci. Eng.* **2011**, *27*, 28.
23. Li, X. The Study of the Eddy Losses and Temperature Field of Winding in Power Transformer. Master's Thesis, Hebei University of Technology, Tianjin, China, 2005.
24. Pan, Y.; Wu, M.; Li, Z. Analysis of Transformer Winding Loss for High-Frequency Switching Power Supply Based on FEM. *Chin. J. Electron Devices* **2012**, *35*, 558–561.
25. Васютинский, С.В. *Transformer Theory and Calculation*, 1st ed.; China Machine Press: Beijing, China, 1983.
26. Jiang, Y.; Lin, Y. Calculation of Eddy Current Losses in Power Transformer Core Clamps. *Electr. Eng.* **2017**, *8*, 25–26.
27. Guerin, C.; Meunier, G.; Tanneau, G. Surface impedance for 3D nonlinear eddy current problems-application to loss computation in transformers. *IEEE Trans. Magn.* **1996**, *32*, 808–811. [CrossRef]
28. Yan, B. Analysis of 3D Leakage Magnetic Field Coupled with Thermal Field in Large Scale Power Transformer. Doctoral Dissertation, Shenyang University of Technology, Shenyang, China, 2012.
29. Zhao, Z.; Wen, T.; Wei, L.; Ji, J.; Li, X. Calculation method of transformer stray loss based on surface impedance boundary. *Chin. J. Sci. Instrum.* **2019**, *40*, 82–89.
30. Liu, J.; Tian, D.; Jing, C.; Wang, J.; Wang, X. Simulation Study on Stray Losses and Temperature Rise in Adjacent Parts of Transformer Ascending Flange. *Tansformer* **2017**, *54*, 14–18.
31. Guo, Z. Research on Eddy Loss and Hot Spot Temperature in Large Transformer Windings. Master's Thesis, Hebei University of Technology, Tianjin, China, 2015.
32. Yin, J. Research on extraction method of winding temperature field distribution characteristics of large oil immersed transformer. *Mach. Electron.* **2022**, *40*, 21–24.
33. Su, X.; Chen, W.; Hu, Q.; Chen, Y.; Pan, C.; Xu, Q. Calculation for transformer winding temperature distribution by numerical analytical technology. *High Volt. Eng.* **2014**, *40*, 3164–3170.
34. Guo, R. Finite Element Analysis and Influence Factors of Heat Dissipation for Discrete Transformer Temperature Field. Master's Thesis, Shandong University, Jinan, China, 2019.
35. Pan, W.; Chen, X.; Zhao, K. Simulation analysis method of hot spot temperature of oil-immersed transformer based on hot spot temperature calculation. *Electr. Meas. Instrum.* **2023**, *44*, 6656–6666.
36. Jiang, H.; Wei, B.; Wen, J.; Dai, M.; Fu, Z.; Liu, Y. Numerical simulation of 3D temperature and flow fields in separated oil-immersed cooling transformer. *High Volt. Appar.* **2021**, *57*, 63–69.
37. Tang, Z.; Qiu, Z.; Liao, C.; Zhou, Y.; Cai, M.; Hao, Y. Influence of External Cooling Modules on Hot-spot Temperature Rise of Distribution Transformer. *High Volt. Appar.* **2022**, *60*, 0135–0143.
38. Schwarzkopf, J.; Cader, T.; Okamoto, K.; Li, B.Q.; Ramaprian, B. Effect of spray angle in spray cooling thermal management of electronics. *Heat Transf. Summer Conf.* **2004**, *46938*, 423–431.
39. Silk, E.A.; Kim, J.; Kiger, K. Spray cooling of enhanced surfaces: Impact of structured surface geometry and spray axis inclination. *Int. J. Heat Mass Transf.* **2006**, *49*, 4910–4920. [CrossRef]
40. Torriano, F.; Chaaban, M.; Picher, P. Numerical study of parameters affecting the temperature distribution in a disc-type transformer winding. *Appl. Therm. Eng.* **2010**, *30*, 2034–2044. [CrossRef]

41. Chereches, N.C.; Chereches, M.; Miron, L.; Hudisteanu, S. Numerical study of cooling solutions inside a power transformer. *Energy Procedia* **2017**, *112*, 314–321. [CrossRef]
42. Alegi, G.L.; Black, W.Z. Real-time thermal model for an oil-immersed, forced-air cooled transformer. *IEEE Trans. Power Deliv.* **1990**, *5*, 991–999. [CrossRef]
43. Mechkov, E.; Tzeneva, R.; Mateev, V.; Yatchev, I. Thermal analysis using 3D FEM model of oil-immersed distribution transformer. In Proceedings of the 2016 19th International Symposium on Electrical Apparatus and Technologies (SIELA), Bourgas, Bulgaria, 29 May–1 June 2016. [CrossRef]
44. Kim, Y.J.; Jeong, M.; Park, Y.G.; Ha, M.Y. A numerical study of the effect of a hybrid cooling system on the cooling performance of a large power transformer. *Appl. Therm. Eng.* **2018**, *136*, 275–286. [CrossRef]
45. Khandan, S.; Tenbohlen, S.; Breuer, C.; Lebreton, R. CFD study of fluid flow and temperature distributions in a power transformer winding. In Proceedings of the 2017 IEEE 19th International Conference on Dielectric Liquids (ICDL), Manchester, UK, 25–29 June 2017. [CrossRef]
46. Mufuta, J.M.; van den Bulck, E. Modelling of the mixed convection in the windings of a disc-type power transformer. *Appl. Therm. Eng.* **2000**, *20*, 417–437. [CrossRef]
47. Skillen, A.; Revell, A.; Iacovides, H.; Wu, W. Numerical prediction of local hot-spot phenomena in transformer windings. *Appl. Therm. Eng.* **2012**, *36*, 96–105. [CrossRef]
48. Lin, L.; Chen, Q.; Chi, M.; Wei, X.; Zhu, X.; Gao, Z. Flow electrification characteristics of typical plane oil-pressboard insulation under AC/DC voltage. In Proceedings of the 2015 IEEE 11th International Conference on the Properties and Applications of Dielectric Materials (ICPADM), Sydney, Australia, 19–22 July 2015. [CrossRef]
49. Chen, Q.; Lin, L.; Gao, Y.; Li, J. Flow electrification characteristics of oil-pressboard insulation under ac superimposed on DC electric field. *IEEE Trans. Dielectr. Electr. Insul.* **2015**, *22*, 2915–2922. [CrossRef]
50. Liu, D.; Liu, N.; Ye, J. Factors Influencing Electrification of Oil Flow in Transformer and Its Suppression Method. *Tansformer* **2024**, *61*, 1–12.
51. Tang, W.H.; Wu, Q.H. *Condition Monitoring and Assessment of Power Transformers Using Computational Intelligence*; Springer Science & Business Media: Berlin/Heidelberg, Germany, 2011.
52. Santisteban, A.; Piquero, A.; Ortiz, F.; Delgado, F.; Ortiz, A. Thermal modelling of a power transformer disc type winding immersed in mineral and ester-based oils using network models and CFD. *IEEE Access* **2019**, *7*, 174651–174661. [CrossRef]
53. Wen, B.; Liu, S.; Feng, J.; Chen, Y. Two dimensional simulation analysis of winding temperature field of oil-immersed power transformer. *Transformer* **2009**, *46*, 35–38.
54. García, A.; Espinosa-Paredes, G.; Hernández, I. A thermal study of an encapsulated electrical transformer. *Comput. Electr. Eng.* **2002**, *28*, 417–445. [CrossRef]
55. Betta, G.; Pietrosanto, A.; Scaglione, A. An enhanced fiber-optic temperature sensor system for power transformer monitoring. *IEEE Trans. Instrum. Meas.* **2001**, *50*, 1138–1143. [CrossRef]
56. Kweon, D.J.; Koo, K.S.; Woo, J.W.; Kwak, J.S. A study on the hot spot temperature in 154kV power transformers. *J. Electr. Eng. Technol.* **2012**, *7*, 312–319. [CrossRef]
57. Takasu, N.; Oshi, T.; Miyawaki, F.; Saito, S.; Fujiwara, Y. An experimental analysis of DC excitation of transformers by geomagnetically induced currents. *IEEE Trans. Power Deliv.* **1994**, *9*, 1173–1182. [CrossRef]
58. Sultan, M.F.; O'Rourke, M.J. Temperature sensing by band gap optical absorption in semiconductors. *Fiber Opt. Laser Sens. XIV* **1996**, *2839*, 191–202. [CrossRef]
59. Grattan, K.T.; Sun, T. Fiber optic sensor technology: An overview. *Sens. Actuators A Phys.* **2000**, *82*, 40–61. [CrossRef]
60. Picanco, A.F.; Martinez, M.L.; Rosa, P.C. Bragg system for temperature monitoring in distribution transformers. *Electr. Power Syst. Res.* **2010**, *80*, 77–83. [CrossRef]
61. Kim, M.; Lee, J.H.; Koo, J.Y.; Song, M. A study on internal temperature monitoring system for power transformer using pptical Fiber Bragg Grating sensors. In Proceedings of the 2008 International Symposium on Electrical Insulating Materials (ISEIM 2008), Yokkaichi, Japan, 7–11 September 2008; pp. 163–166. [CrossRef]
62. McNutt, W.J.; McIver, J.C.; Leibinger, G.E.; Fallon, D.J.; Wickersheim, K.A. Direct measurement of transformer winding hot spot temperature. *IEEE Trans. Power Appar. Syst.* **1984**, *PAS-103*, 1155–1162. [CrossRef]
63. Xin, S.J.; Chai, W. Study on encapsulating method of FBG temperature sensor. *J. Transducer Technol.* **2004**, *23*, 10–12.
64. Ribeiro, A.L.; Eira, N.F.; Sousa, J.M.; Guerreiro, P.T.; Salcedo, J.R. Multipoint fiber-optic hot-spot sensing network integrated into high power transformer for continuous monitoring. *IEEE Sens. J.* **2008**, *8*, 1264–1267. [CrossRef]
65. Qi, Y.; Wu, G.; Wang, Y. Optimum design of fiber Bragg grating real-time online temperature detecting sensor for power cable. *J. Cent. South Univ. (Sci. Technol.)* **2011**, *42*, 3415–3420.

66. Wang, E.; Zhao, Z.; Cao, M.; Tang, B.; Li, C. Multi point temperature monitoring of oil immersed transformer based on fiber Bragg grating. *High Volt. Eng.* **2017**, *43*, 1543–1549.
67. Yilmaz, G.; Karlik, S.E. A distributed optical fiber sensor for temperature detection in power cables. *Sens. Actuators A Phys.* **2006**, *125*, 148–155. [CrossRef]
68. Mandal, J.; Pal, S.; Sun, T.; Grattan, K.T.; Augousti, A.T.; Wade, S.A. Bragg grating-based fiber-optic laser probe for temperature sensing. *IEEE Photonics Technol. Lett.* **2004**, *16*, 218–220. [CrossRef]
69. Lee, Y.W.; Yoon, I.; Lee, B. A simple fiber-optic current sensor using a long-period fiber grating inscribed on a polarization-maintaining fiber as a sensor demodulator. *Sens. Actuators A Phys.* **2004**, *112*, 308–312. [CrossRef]
70. Cusano, A.; Cutolo, A.; Nasser, J.; Giordano, M.; Calabro, A. Dynamic strain measurements by fibre Bragg grating sensor. *Sens. Actuators A Phys.* **2004**, *110*, 276–281. [CrossRef]
71. Berkoff, T.A.; Kersey, A.D. Experimental demonstration of a fiber Bragg grating accelerometer. *IEEE Photonics Technol. Lett.* **1996**, *8*, 1677–1679. [CrossRef]
72. Jones, S.; Bucea, G.; McAlpine, A.; Nakanishi, M.; Mashio, S.; Komeda, H.; Jinno, A. Condition monitoring system for TransGrid 330 kV power cable. In Proceedings of the 2004 International Conference on Power System Technology, 2004. PowerCon 2004, Singapore, 21–24 November 2004. [CrossRef]
73. Jiang, Q.; Sui, Q. Technological study on distributed fiber sensor monitoring of high voltage power cable in seafloor. In Proceedings of the 2009 IEEE International Conference on Automation and Logistics, Shenyang, China, 5–7 August 2009. [CrossRef]
74. Lee, J.H.; Kim, S.G.; Park, H.J.; Song, M. Investigation of Fiber Bragg Grating temperature sensor for applications in electric power systems. In Proceedings of the 2006 IEEE 8th International Conference on Properties & applications of Dielectric Materials, Bali, Indonesia, 26–30 June 2006. [CrossRef]
75. Cooney, W.H. Predetermination of self-cooled oil-immersed: Transformer temperatures before conditions are constant. *J. AIEE* **1925**, *44*, 1324–1331. [CrossRef]
76. *IEEE Std C57.91-2011 (Revision of IEEE Std C57.91-1995)*; IEEE Guide for Loading Mineral-Oil-Immersed Transformers and Step-Voltage Regulators. Institute of Electrical and Electronics Engineers: New York, NY, USA, 2012.
77. *IEC 60076-7-2005*; Power Transformers—Part 7: Loading Guide for Oil-Immersed Power Transformers. International Electrotechnical Commission: Geneva, Switzerland, 2005.
78. Swift, G.; Molinski, T.S.; Lehn, W. A fundamental approach to transformer thermal modeling. I. Theory and equivalent circuit. *IEEE Trans. Power Deliv.* **2001**, *16*, 171–175. [CrossRef]
79. Swift, G.; Molinski, T.S.; Bray, R.; Menzies, R. A fundamental approach to transformer thermal modeling. II. Field verification. *IEEE Trans. Power Deliv.* **2001**, *16*, 176–180. [CrossRef]
80. Galdi, V.; Ippolito, L.; Piccolo, A.; Vaccaro, A. Parameter identification of power transformers thermal model via genetic algorithms. *Electr. Power Syst. Res.* **2001**, *60*, 107–113. [CrossRef]
81. Pierce, L.W. Predicting liquid filled transformer loading capability. In Proceedings of the 1992 Record of Conference Papers Industry Applications Society 39th Annual Petroleum and Chemical Industry Conference, San Antonio, TX, USA, 28–30 September 1992. [CrossRef]
82. Jiang, T.; Li, J.; Chen, W.; Sun, C.; Zhao, T. Thermal model for hot spot temperature calculation in oil-immersed transformers. *High Volt. Eng.* **2009**, *35*, 1635–1640.
83. Gastelurrutia, J.; Ramos, J.C.; Larraona, G.S.; Rivas, A.; Izagirre, J.; Del Río, L. Numerical modelling of natural convection of oil inside distribution transformers. *Appl. Therm. Eng.* **2011**, *31*, 493–505. [CrossRef]
84. Jiang, B.N. *The Least-Squares Finite Element Method: Theory and Applications in Computational Fluid Dynamics and Electromagnetics*; Springer Science & Business Media: Berlin/Heidelberg, Germany, 1998.
85. Yu, S.T.; Jiang, B.N.; Liu, N.S.; Wu, J. The least-squares finite element method for low-mach-number compressible viscous flows. *Int. J. Numer. Methods Eng.* **1995**, *38*, 3591–3610. [CrossRef]
86. Taghikhani, M.A.; Gholami, A. Prediction of hottest spot temperature in power transformer windings with non-directed and directed oil-forced cooling. *Int. J. Electr. Power Energy Syst.* **2009**, *31*, 356–364. [CrossRef]
87. Chen, W.; Su, X.; Sun, C.; Pan, C.; Tang, J. Temperature distribution calculation based on FVM for oil-immersed power transformer windings. *Electr. Power Autom. Equip.* **2011**, *31*, 23–27.
88. Tsili, M.A.; Amoiralis, E.I.; Kladas, A.G.; Souflaris, A.T. Power transformer thermal analysis by using an advanced coupled 3D heat transfer and fluid flow FEM model. *Int. J. Therm. Sci.* **2012**, *53*, 188–201. [CrossRef]
89. Wang, Y.; Ma, L.; Lv, F.; Bi, J.; Wang, L. Calculation of 3D temperature field of oil immersed transformer by the combination of the finite element and finite volume method. *High Volt. Eng.* **2014**, *40*, 3179–3185.
90. Li, J.; Gu, S.; Wang, Y.; Ye, X.; Wu, H.; Liu, H. Study on influencing factors of converter transformer hot spot temperature based on finite element method. *Electron. Test* **2022**, *19*, 76–92.

91. Yuan, F.; Shi, W.; Wang, Y.; Chen, W.; Tang, B.; Jiang, L. Temperature characteristic analysis and radiator optimization of oil-immersed transformer based on multi-physical field simulation. *High Volt. Eng.* **2024**, *50*, 221–231.
92. Alvarez, D.L.; Rivera, S.R.; Mombello, E.E. Transformer thermal capacity estimation and prediction using dynamic rating monitoring. *IEEE Trans. Power Deliv.* **2019**, *34*, 1695–1705. [CrossRef]
93. Wang, J. The Method Research on Hot-Spot Temperature Prediction Andlocation for Oil-Immersed Transformer. Doctoral Dissertation, Southwest Jiaotong University, Chengdu, China, 2020.
94. Yang, C. Research on Temperature Characteristics and Hot Spot Temperature Prediction of Oil-Immersed Transformer. Doctoral Dissertation, Nanjing University of Posts and Telecommunications, Nanjing, China, 2023.
95. Yuan, F.; Shi, W.; Wang, Y. Real-time Prediction Method of Hot Spot Temperature of Oil-Immersed Transformer Based on Flow-thermal Coupling Simulation and EEMD-LSTM Network. *High Volt. Eng.* **2024**, 1–14.
96. Kumbhar, G.B.; Kulkarni, S.V. Analysis of short-circuit performance of split-winding transformer using coupled field-circuit approach. *IEEE Trans. Power Deliv.* **2007**, *22*, 936–943. [CrossRef]
97. Li, X.; Chen, Q.; Hu, G.; Sun, J.; Long, G. Numerical analysis on magnetic field of HTS transformer with different geometry. *IEEE Trans. Magn.* **2006**, *42*, 1343–1346. [CrossRef]
98. Jing, Y. Study of Oil Flow Distribution and Winding Temperature Field in Large Power Transformers. Doctoral Dissertation, Shenyang University of Technology, Shenyang, China, 2014.
99. Li, L.; Cui, X.; Zhang, Y.; Cheng, Z. Calculation of the 3d nonlinear magnetic field and eddy current loss of the plate in transformer. *Proc. CSEE* **1999**, *19*, 33–36.
100. Gong, L. Analysis on Magnetic Leakage and Eddy Current Loss of Metal Structure of Power Transformer. Master's Thesis, Harbin University of Science and Technology, Harbin, China, 2013.
101. Li, Y.; Eerhemubayaer; Zhang, X.; Jing, Y.; Li, X. Magnetic-thermal coupling calculation and shielding measure of local overheating for transformer. *J. Shenyang Univ. Technol.* **2012**, *34*, 366–371.
102. Hu, Y. Research on the Leakage Magnetic Fields and Local Overheating Due to the Magnetic Shunt and Heavy Current Leads in Large Power Transformers. Doctoral Dissertation, Shenyang University of Technology, Shenyang, China, 2001.
103. Ho, S.L.; Li, Y.; Tang, R.Y.; Cheng, K.W.E.; Yang, S.Y. Calculation of eddy current field in the ascending flange for the bushings and tank wall of a large power transformer. *IEEE Trans. Magn.* **2008**, *44*, 1522–1525. [CrossRef]
104. Jing, Y.; Li, Y. Eddy current losses calculation and shields of high voltage auto-transformer. *High Volt. Eng.* **2012**, *38*, 1988–1994.
105. Xiao, R. Temperature Field Simulation Modeling and Rapid Prediction Method of Real-time Temperature of Converter Transformer. Doctoral Dissertation, Chongqing University, Chongqing, China, 2022.
106. Choi, C.; Yoo, H.S.; Oh, J.M. Preparation and heat transfer properties of nanoparticle in transformer oil dispersions as advanced energy-efficient coolants. *Curr. Appl. Phys.* **2008**, *8*, 710–712. [CrossRef]
107. Nazari, M.; Jafarmadar, S.; Gohery, S. Convective heat transfer behavior and AC dielectric breakdown voltage of electric power transformer oil with magnetic colloidal nano-fluid: An experimental study. *Case Stud. Therm. Eng.* **2023**, *45*, 103017. [CrossRef]
108. Wang, B. Study on Multiphysical Properties of Traction Transformer Insulation Modification Based on Molecular Simulation. Master's Thesis, Shenyang University of Technology, Shenyang, China, 2023.
109. Khudhair, A.A.; Jabal, M.H.; Ismail, S.J. Corn oil performance's a bio cooling fluid in electric distribution transformer. *Eng. Technol. J.* **2022**, *40*, 20–30. [CrossRef]
110. Shen, W. Research on Heat Transfer Performance of Large Oil Immersed Natural Ester Oil Transformer. Master's Thesis, Hebei University of Science and Technology, Hebei, China, 2023.
111. Ma, B.; Chen, X.; Zheng, Y.; Liu, K.; Tao, Z.; Peng, R.; Wang, B.; Yuan, J. Research Progress and Trends of Eco-Friendly Insulating Oil for Power Transformers. *South. Power Syst. Technol.* **2024**, *18*, 12–21.
112. Zhu, X.; Liu, Z.; Li, S. Simulation analysis of temperature rise characteristics of oil-immersed transformer based on fluid-hot spot temperature coupling. *Electr. Eng.* **2022**, *15*, 46–50. [CrossRef]
113. Wang, F. Research Leakage Magnetic Field and Analyze Winding Temperature Field for Power Transformer. Master's Thesis, Harbin University of Science and Technology, Harbin, China, 2014.
114. Hosseini, R.; Nourolahi, M.; Gharehpetian, G.B. Determination of OD cooling system parameters based on thermal modeling of power transformer winding. *Simul. Model. Pract. Theory* **2008**, *16*, 585–596. [CrossRef]
115. Rahimpour, E.; Barati, M.; Schäfer, M. An investigation of parameters affecting the temperature rise in windings with zigzag cooling flow path. *Appl. Therm. Eng.* **2007**, *27*, 1923–1930. [CrossRef]
116. Jiang, Q.; Zhu, Z.; Zhang, Q. Optimal design of the first stage of the plate-fin heat exchanger for the EAST cryogenic system. *Plasma Sci. Technol.* **2018**, *20*, 035601. [CrossRef]
117. Liu, J.C.; Zhang, S.Y.; Zhao, X.Y.; Yi, G.D.; Zhou, Z.Y. Influence of fin arrangement on fluid flow and heat transfer in the inlet of a plate-fin heat exchanger. *J. Zhejiang Univ.-Sci. A* **2015**, *16*, 279–294. [CrossRef]
118. Wen, J.; Li, K.; Liu, Y.; Wu, M.; Wang, S.; Li, Y. Multi-Objective Optimization of Serrated Fin in Plate-Fin Heat Exchanger by Fluid Structure Interaction. *J. Xi'an Jiaotong Univ.* **2018**, *52*, 130–135.

119. Peng, X.; Liu, Z.; Qiu, C.; Tan, J. Effect of inlet flow maldistribution on the passage arrangement design of multi-stream plate-fin heat exchanger. *Appl. Therm. Eng.* **2016**, *103*, 67–76. [CrossRef]
120. Wang, Y. Numerical Analysis of Winding Temperature Field for Large Oil-Immersed Transformer Based on COMSOL. Master's Thesis, Hebei University of Technology, Hebei, China, 2021.

Disclaimer/Publisher's Note: The statements, opinions and data contained in all publications are solely those of the individual author(s) and contributor(s) and not of MDPI and/or the editor(s). MDPI and/or the editor(s) disclaim responsibility for any injury to people or property resulting from any ideas, methods, instructions or products referred to in the content.